

## Microstructure and mechanical properties of $\text{TiB}_2/(\text{Cu}, \text{Ni})$ interpenetrating phase composites

Xinghong Zhang,<sup>a,b</sup> Changqing Hong,<sup>a,\*</sup> Jiecai Han<sup>a</sup> and Hexin Zhang<sup>a</sup>

<sup>a</sup>Center for Composite Materials, Harbin Institute of Technology, Harbin 150001, PR China

<sup>b</sup>Anhui University of Technology and Science, Wuhu 241000, PR China

Received 16 September 2005; revised 5 April 2006; accepted 17 April 2006

Available online 23 June 2006

$\text{TiB}_2/(\text{Cu}, \text{Ni})$  interpenetrating phase composites (IPCs) with ceramic volume content of 75–86% were prepared by melt infiltration. The microstructure of  $\text{TiB}_2/(\text{Cu}, \text{Ni})$  IPCs is characterized by the three-dimensional interpenetration of  $\text{TiB}_2$  and Cu–Ni phases. Bending strength and fracture toughness of CuNi/81.6% $\text{TiB}_2$  IPCs are as high as 640.5 MPa and 9.37 MPa  $\text{m}^{1/2}$ , respectively. The combination of the micro-crack and interfacial debonding and the cleavage of  $\text{TiB}_2$  grains are the main fracture modes of  $\text{TiB}_2/\text{Cu}$ –Ni IPCs. © 2006 Acta Materialia Inc. Published by Elsevier Ltd. All rights reserved.

**Keywords:** Interpenetrating phase composite; Melt infiltration; Microstructure; Fracture

Recently research has progressed from traditional composite materials with discrete, dispersed additions and has focused on incorporating larger quantities of second phase reinforcements or the utilization of processing routes that result in composites with a connected second phase [1,2]. This new class of composite materials has been termed interpenetrating phase composites (IPCs) and has attracted much interest over the past 10 years [3–5]. Interpenetrating phase composites (IPCs) represent a family of materials whose microstructures are characterized by the continuity and interpenetration of two or more phases. In the context of ceramic–metal IPCs, much of the driving force for investigating interpenetrating microstructures has been the toughening of ceramics by addition of low concentrations of a metal phase. Therefore, IPCs of 60 vol.% ceramic or more are most common in the literature [6,7].

This new material is the subject of much interest in regard to lightweight structural, wear resistant components and/or armored applications. Presently, the  $\text{Al}_2\text{O}_3$ –metal (Al, Cu) [8,9], TiC–metal (Ni, Mg) [10] or TiC–intermetallic (FeAl, NiAl,  $\text{Ni}_3\text{Al}$ ) [11–13] systems are proving to be interesting IPCs for either theoretical studies or practical applications. However, studies on  $\text{TiB}_2$ –metal or alloys IPCs are very limited.

$\text{TiB}_2$  is attractive for high temperature applications because of its high hardness at high and low temperature environments, high melting point (3253 K), high ther-

mal and electric conductivity, good chemical stability and good thermal shock stability. Several recent reviews [14,15] give general methods to enhance the wettability in metal–nonmetal systems. The wetting angle of noble and base metals on oxide ceramics can be decreased significantly by small additions of alloy element. Previous studies showed that addition of an alloy element such as Ni or Al can improve the wettability of  $\text{TiB}_2$  ceramic and Cu metal (the wettability angle of  $\text{TiB}_2/\text{Cu}$  is 140° in vacuum [16]).

Many techniques have been found to prepare ceramic–metal IPCs, e.g., the pressure regulated melt infiltration process [12], pressureless melt infiltration of a pre-sintered preform [10], the self-propagating high temperature synthesis [17] and so on. Of the many methods, pressureless melt infiltration is particularly interesting because it offers the advantages of low cost, ease of composite production and near net shape capability. In the present study pressureless melt infiltration was adopted to prepare fully dense  $\text{TiB}_2/\text{Cu}$ –Ni IPCs with high  $\text{TiB}_2$  content (75–86 vol.%), and the interpenetrating microstructure and mechanical properties were investigated in detail.

The constituent materials used in the present study were  $\text{TiB}_2$  powder produced by the Northwest Institute for Non-Ferrous Metal Research, Xi'an, China with a mean particle size of 2  $\mu\text{m}$ , and commercial nickel powder (70–100  $\mu\text{m}$ ) and copper powder (70–100  $\mu\text{m}$ ).

$\text{TiB}_2$  powder was de-agglomerated in 2-propanol medium with WC/Co balls, then dried and sieved through an 80-mesh sieve before forming.  $\text{TiB}_2$  preforms were first

\* Corresponding author. E-mail: [hongcq@hit.edu.cn](mailto:hongcq@hit.edu.cn)

pressed by filling a cuboid-shaped rubber mould with suitable amounts of  $\text{TiB}_2$  powder, followed by cold isostatic pressing up to 200 MPa (giving  $\text{TiB}_2$  green densities of 50–70% of theoretical). The green-compact billets were sintered in a furnace, in a vacuum atmosphere, at a heating rate of  $10\text{ }^\circ\text{C}/\text{min}$ . The sintering temperature was from  $1700\text{ }^\circ\text{C}$  to  $2000\text{ }^\circ\text{C}$ . All specimens were held at the sintering temperature for 30 min and then cooled to room temperature at the same rate of  $10\text{ }^\circ\text{C}/\text{min}$ . A predetermined amount of Cu–Ni powder was placed on the  $\text{TiB}_2$  pellets, which were positioned on high-purity  $\text{Al}_2\text{O}_3$  powder (99.99%) within a high-purity graphite furnace under a dynamic vacuum of  $\sim 10^{-1}\text{ Pa}$ , at  $1400\text{ }^\circ\text{C}$  and  $1500\text{ }^\circ\text{C}$ , and the conditions were maintained for 60 min. The above different preforms were infiltrated with Cu–Ni in an indirect downward infiltration mode in the present study, which is schematically illustrated in Figure 1.

Figure 2 shows the microstructures of porous  $\text{TiB}_2$  specimens sintered from different compacts at a temperature of  $2000\text{ }^\circ\text{C}$ . Interpenetrating voids and small flaws existed in the specimen, due to a loose connection between the  $\text{TiB}_2$  grains. However, these voids and small flaws were reduced greatly with the increasing initial compact density, indicating a better connection between the  $\text{TiB}_2$  grains. It can be seen that highly packed regions densified faster than the less-dense regions, as shown in Figure 2(a) and (b), where the ceramic grains clearly have grown in the neck area but the connections between the particles are still porous structures.

Figure 3 shows the dependence of relative density on the sintering temperature of the  $\text{TiB}_2$  porous network. It can be seen that for the lower density initial green compacts, higher temperatures are required to reach the same density as that of the green compact with higher density.

Figure 4(a) and (b) shows typical micrographs of  $\text{TiB}_2/\text{Cu-Ni}$  prepared by spontaneously infiltrating the  $\text{TiB}_2$  preforms of the two groups with  $\text{TiB}_2$  volume content of 75.5% and 86.4%, respectively. It should be noted that the bright phase is Cu–Ni, and the black is  $\text{TiB}_2$  by energy dispersive X-ray spectroscopy analysis. The bond between  $\text{TiB}_2$  and Cu–Ni looked good and strong. No obvious micro-defects such as large voids and separated

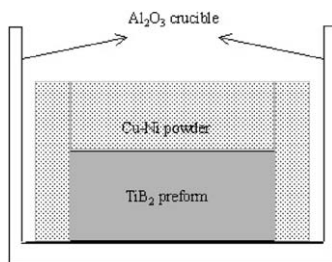


Figure 1. Scheme of indirect downward horizontal infiltration.

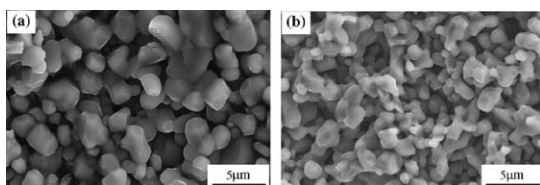


Figure 2. SEM micrographs of  $\text{TiB}_2$  specimens sintered from (a) porosity 32.5% and (b) porosity 28.4% at  $2000\text{ }^\circ\text{C}/1\text{ h}$ .

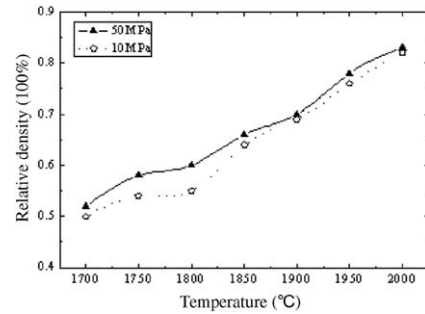


Figure 3. Dependence of relative density on sintering temperature of  $\text{TiB}_2$  porous network.

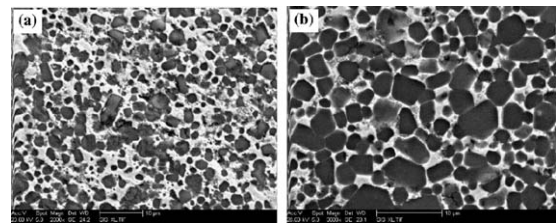


Figure 4. Typical micrographs of  $\text{TiB}_2/\text{Cu-Ni}$  composites infiltrated at  $1500\text{ }^\circ\text{C}$ : (a) with 75.5 vol.%  $\text{TiB}_2$ , (b) with 86.4 vol.%  $\text{TiB}_2$ , prepared by infiltrating the  $2000\text{ }^\circ\text{C} \times 1\text{ h}$  pre-sintered  $\text{TiB}_2$  preform.

interface of  $\text{TiB}_2$  and Cu–Ni were observed. The infiltration ability of liquid Cu–Ni in porous  $\text{TiB}_2$  preform was adequate to form fully dense and defect-free composites. It is interesting to see in Figure 4 that  $\text{TiB}_2$  particles join each other. The joints between  $\text{TiB}_2$  particles formed in the pre-sintering stage and were maintained after infiltration. Cu–Ni melt filled the channels within the three-dimensional network of the joining  $\text{TiB}_2$  particles and formed also a continuous network of Cu–Ni.

Slightly higher densities were generally observed for materials processed at  $1500\text{ }^\circ\text{C}$  when compared to those processed at  $1400\text{ }^\circ\text{C}$  (shown in Fig. 5), particularly for the lowest binder contents (i.e.,  $<20\text{ vol.}\%$ ). These materials exhibited minimal porosity for Cu–Ni contents of  $>20\text{ vol.}\%$ , with retained pore sizes generally being sub-micrometer in magnitude.

Table 1 lists the mechanical properties of the prepared  $\text{TiB}_2/\text{Cu-Ni}$  IPCs. The  $\text{TiB}_2$  volume fraction of the composite was estimated from the density of the composites, which was measured by the Archimedes method in ethylene glycol, and is given by the following equation:

$$\rho_{(\text{Cu,Ni})} \times \rho_{\text{TD}}(1 - V_{\text{TiB}_2}) + \rho_{\text{TiB}_2} \times \rho_{\text{TD}} \times V_{\text{TiB}_2} = d_{\text{measured}} \quad (1)$$

$$\rho_{(\text{Cu,Ni})} = \frac{m}{\frac{m_{\text{Cu}}}{\rho_{\text{Cu}}} + \frac{m_{\text{Ni}}}{\rho_{\text{Ni}}}} \quad (2)$$

where  $\rho_{(\text{Cu,Ni})}$  and  $\rho_{\text{TiB}_2}$  are the densities of Cu–Ni alloy and  $\text{TiB}_2$ , respectively. The  $\rho_{\text{TD}}$  represents the relative density of the  $\text{TiB}_2/\text{Cu-Ni}$  composites. The density of Cu–Ni can be calculated from Eq. (2). In this study, 8.93 and  $4.52\text{ g}/\text{cm}^3$ , respectively, are taken as the densities of Cu–Ni and  $\text{TiB}_2$ . From Eq. (1) and Eq. (2), the calculated volume fraction of  $\text{TiB}_2$  in the composites is as listed in Table 1. We can see that the calculated volume fraction of  $\text{TiB}_2$  after infiltration is higher than that of the preforms before infiltration. A major reason that caused the  $\text{TiB}_2$  content to increase a little is that the

Download English Version:

<https://daneshyari.com/en/article/1503511>

Download Persian Version:

<https://daneshyari.com/article/1503511>

[Daneshyari.com](https://daneshyari.com)